

Emission Measurements of Various Biofuels using a Commercial Swirl-Type Air-Assist Dual Fuel Injector

Joachim Agou^{*}, Alain deChamplain[†], and Bernard Paquet[‡]

Combustion Laboratory, Mechanical Engineering Department, Université Laval, Quebec City, QC, G1V 0A6

Abstract

A joint university-industry research program funded by Rolls-Royce Canada, NSERC and CRIAQ is actually pursued at Université Laval to characterize the combustion performance of liquid (biodiesel blends) and gaseous (syngas blends) biofuels in terms of emissions & smoke and lean blow out. The final objective of the proposed research is to characterize the most promising liquid and gaseous novel biofuels for use in industrial gas turbines in order to reduce greenhouse gases and potentially operation costs. These combustion tests allowed the characterization of standard diesel fuel as a baseline plus two biodiesel blends as well as standard methane as a baseline plus ten syngas blends (CH₄, H₂, CO and CO₂) in order to evaluate the emissions of the main pollutants (CO, CO₂, NO_x, UHCs and smoke). Combustor exit and wall temperature measurements were also taken to characterize adequately the boundary conditions for future CFD simulations. The flame was contained in a quartz tube combustor operating at ambient outlet conditions and the fuel was delivered through a commercial swirl-type, airblast dual fuel atomizer. The air mass flow rate was kept constant for all fuels to maintain the same pressure drop (ΔP) across the fuel injector while the fuel flow was varied to cover equivalence ratios from 0.5 to 1. A probe connected to a FTIR/FID/O₂ gas analyzer system and a smoke filter was fixed to a 3D-axis traverse in order to sample combustion products in a cross pattern at the combustor exit. This way, concentrations of various emissions were obtained at five radial positions. Burned gases and wall temperatures were measured with thermocouples along the test rig. This paper reports the findings of these experimental tests and presents the comparisons of the biofuels with baseline fuels to identify some benefits of these novel biofuels while maintaining an acceptable overall combustion performance.

1. Introduction

As sources of fossil fuels are diminishing in the world, energy security, self-reliance and environmental impact have become important issues for the combustion science community as well as the general population. To remedy those issues, several biologically sourced fuels such as syngas, biogas, and biodiesel, have been identified as suitable candidates to be used in combustion devices due to their favorable availability and potentially better emissions. Such biologically derived fuels are more sustainable since their sources can be grown, making their use an excellent way to offset the carbon emitted due to combustion activities.

Over many decades of combustion research, a good knowledge base was assembled for conventional fossil fuels with regards to combustion characteristics. A similar knowledge base for biologically sourced fuels is now required since lacking for most of these alternative fuels. Without this knowledge base, it would be very difficult to design properly a gas turbine combustor that would use these alternative fuels efficiently while producing fewer pollutants compared to the use of fossil fuels [1]. This paper reports the findings of these experimental tests and presents the comparisons of alternative fuels with baseline fuels to identify the benefits of these novel biofuels.

2. Experimental Setup

The liquid and gaseous fuelled swirl-flame burner used for the current research was further developed from an existing design in the combustion laboratory at Université Laval. It consists of a stainless steel base plate mounted on an inlet manifold and with the whole assembly installed on a support bolted to the floor (Fig. 1). To represent the primary zone of a gas turbine combustor, the combustion chamber is confined in a quartz tube that a 110 mm inside diameter and a 300 mm height. This quartz tube enables almost unrestricted optical access to the flame which fires vertically during the tests. The base plate with manifold is adapted to mount the swirl-type air-assist fuel injector coming from a commercial Trent 60 WLE DF gas turbine provided by Rolls-Royce Canada (RRC). This air-assist atomizer has high swirl as well as dual fuel (DL) capabilities. Its double inlet can deliver gaseous or liquid fuels by their own path. To summarize his purpose, this atomizer employs a simple concept whereby fuel at low pressure is arranged to flow over a lip located in a high-velocity airstream. As the fuel flows over the lip, it is atomized by the air, which then enters the combustion zone carrying the fuel droplets (if liquid fuel) for evaporation and mixing. An ignition module is incorporated to the test rig in order to facilitate flame initiation particularly essential in the use of diesel and biodiesel blends. Consequently, next to the fuel injector, an independent propane inlet is installed with a sparking electrode (~35 kV) that serves as a pilot flame to the combustor. K-type thermocouples measure temperature at different locations on the rig during the tests. Burned gas temperature is measured at the center of the exit plane of the quartz tube as well as wall temperatures at several locations along the test rig.



Figure 1: Custom test rig.

^{*}Graduate student

[†]Research Associate

[‡]Professor and corresponding author, alain.dechamplain@gmc.ulaval.ca

To measure the air supplied from the university compressor and the liquid fuel pump, high precision Coriolis flow meters are used to regulate accurately the main air and liquid fuel flow rates. Concerning the gaseous fuel, high precision mass flow controllers are used to mix and regulate the different biogas and syngas mixtures coming from high pressure cylinders. Finally a stainless steel cone which serves as a restriction at the exit to simulate the pressure drop generated by the turbine stage is mounted atop the quartz tube and held in place with threaded rods.

3. Instrumentation

The combustion laboratory Université Laval is equipped with state-of-the-art analysers for the measurement and analysis of gas turbine emissions. A stainless steel probe (6,4 mm D tube) connected to a gas analyzer system (and a smoke filter) is mounted on a 3D-axis traverse that allows displacement of the probe with high accuracy at different locations in the exit plane. Samples of combustion products are drawn in a cross pattern at the combustor exit. Instrumentation (Fig. 2) allows monitoring of the air and fuel mass flows, inlet air temperature and pressure, combustor wall temperatures, and exhaust gas composition.

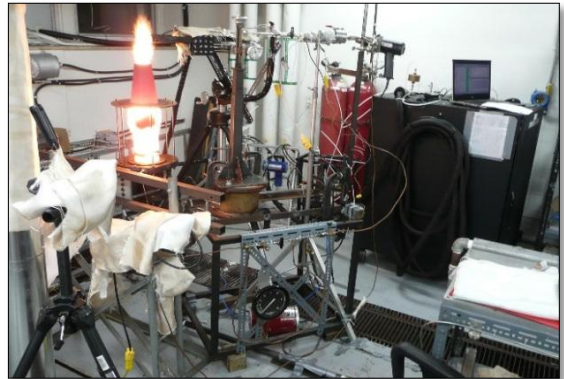


Figure 2: Experimental instrumentation.

3.1 Smoke Measurements

A designed smoke sampler is used to determinate the smoke number (SN) following the SAE procedure found in Aerospace Recommended Practice ARP1179. The soot samples are collected by passing a predetermined volume of undiluted exhaust sample at a certain flow rate through a specific type of paper filters (Fig. 3) via a heated line (150°C) to prevent condensation. A reflectometer (ANSI) is used to measure the absolute reflectance of the clean filter paper as well as the stained filter to calculate the smoke number (SN).



Figure 3: Stained paper filters.
(Diesel @ $\phi = 0.8, 0.9, 1$)

3.2 Gaseous Emissions

Most gaseous emissions are quantified using a Gasmet™ Continuous Emission Monitoring System (CEMS) Fourier Transform Infrared (FTIR)-based gas analyzer (Fig. 4). The analyzer quantifies gas species concentrations by measuring the absorption of an emitted infrared light source through the gas sample.

Molecules in gas phase vibrate and rotate at frequencies characteristic to each molecule. Each frequency is associated with an energy state of a molecule. Infrared radiation moves the molecules to higher energy states; characteristic frequencies are absorbed by the molecule in the process. Each molecule absorbs infrared radiation at several characteristic frequencies or wavelengths. The result is an IR absorption spectrum: a fingerprint unique to each molecule. All molecules can be identified on the basis of their characteristic absorption spectrum except diatomic elements such as O₂ and noble gases. Each molecule absorbs infrared radiation at its characteristic wavelength. Absorption strength is directly proportional to concentration (Beer's law).

This analyzer can simultaneous analyse up to 35 gaseous substances like H₂O, CO₂, CO, SO₂, NO, NO₂, N₂O, HF, NH₃, O₂, O₃, and many HC volatiles. An industrial PC is used to process and store the sample spectra with the CALCMET™ software provided by the gas analyser manufacturer. The software analyzes the sample spectrum using sophisticated multicomponent algorithms and is capable of simultaneous detection, identification and quantification of the gas components. Cross-interference effects are compensated and accuracy is maintained even when analyzing complex gas mixtures where there is a possibility of spectral overlap. As the FTIR gas analyzer cannot detect diatomic molecules, an ENOTEC™ (Zr - O₂) oxygen analyzer was added. A Siemens™ Fidamat 6-G Flame Ionization Detector (FID) that measures total hydrocarbon concentrations (THCs) with high accuracy since THCs with a FT-IR is not yet an accepted value for missing HCs.



Figure 4: CEMS cabinet.

3.3 Fuel Characteristics

To perform the experimental tests with liquid fuels, biodiesel/diesel blends are used. The blends considered in the experiment are: Diesel as a baseline, B20, B50 and B100 as shown in Table 1.

To characterize a wide range of bio-based gaseous fuels, eleven different fuel compositions are considered in this study. The compositions include one biogas composition (B1), seven syngas compositions with H₂/CO ratios

ranging from 0.5 to 2 (S1-S6, S14), and two syngas/methane blends with 25% and 50% by volume added methane: S5M25 which is 75% S5 with 25% CH₄ or S5M50 which is 50% S5 with 50% CH₄. The biogas B1 contains 60% CH₄ and 40% CO₂ and is a typical biogas from digesters. The three syngas compositions S1, S2, and S3 have a fixed CO₂ content (25%) and no methane, but the H₂/CO ratio varies from 0.5 to 2. The syngas compositions S4, S5, and S6 are similar to S1, S2, and S3, but 5% methane is added (close to the average content of methane for most sources of syngas) and the CO₂ content is reduced slightly to allow for this. The S14 syngas composition has a reduced CO₂ content (15%) and contains no methane. The S5 syngas composition, having 5% methane and a H₂/CO ratio of unity was blended to ratios of 75:25 and 50:50 with pure methane leading to the S5M25 and S5M50 compositions. These selected compositions allow for the effects of hydrogen, methane, and carbon dioxide content to be explored and the role of the constituents on syngas combustion to be examined. Moreover, as syngas can be blended with natural gas in many applications, the selected blends with methane also allow for combustion properties of syngas/natural gas blends to be examined. It should be expected that each of these gaseous biofuels will burn in a unique way and generate a range of combustion products of varying composition [2].

Table 1: List of fuels tested during this study

Liquid Fuels		Diesel No.2 (% vol.)			Bio-diesel (% vol.)		
<i>Diesel (baseline)</i>		100			0		
B20		80			20		
B50		50			50		
B100		0			100		
Gaseous Fuels		H ₂ /CO ratio	CO (% vol.)	H ₂ (% vol.)	CH ₄ (% vol.)	CO ₂ (% vol.)	N ₂ (% vol.)
<i>Biogas (baseline)</i>			0	0	100	0	0
B1		-	0	0	60	40	0
S1		0.5	50	25	0	25	0
S2		1.0	37.5	37.5	0	25	0
S3		2.0	25	50	0	25	0
S4		0.5	50	25	5	20	0
S5		1.0	37.5	37.5	5	20	0
S6		2.0	25	50	5	20	0
S14		1.0	42.5	42.5	0	15	0
S5M50		1.0	18.75	18.75	52.5	10	0
S5M25		1.0	28.125	28.125	28.75	15	0

3.4 Test conditions and Procedure

In order to maintain operating conditions with a 3.5% pressure drop through the injector, the required constant mass flow rate of air is calculated at 23.6 g/s. The air mass flow rate being constant for all conditions, the fuel flow rates are from a stoichiometric equivalent ratio ($\phi = 1$) to reach lean blowoff ($0.3 < \phi < 0.5$) depending on fuels types. In order to find a fair compromise between experimental accuracy and fuel cost, it was decided to measure 5 points at the exit plane for each equivalence ratio: 1 at the center and 4 around the circumference at a 2 cm radial position to get decent emission profiles. Each data point comprises 3 gas analyzer and 3 smoke measurements with verification for consistency and compliance then averaged to obtain one value of smoke and



Figure 6: B1 gas at $\phi=1$.

emissions. The time required to measure is about 5 min for emissions and 10 min for soot. Smoke was not measured for the gaseous fuels because it was negligible and to reduce high fuel consumptions. Finally, it took several months to complete the whole experimental program to adapt the different experimental configurations required for each fuel, and the several issues and challenges for the handling of compressed gases to produce the different gas mixtures.

4. Discussion and Results

As with any fuel, the combustion of liquid (Fig. 5) or gaseous biofuels (Fig. 6) can produce gaseous pollutants such as nitrogen oxides (NO_x), carbon monoxide (CO), sulfur dioxide (SO₂), volatile organic compounds (VOCs), and particulate matter. The amount of emissions generated depends on the properties of the fuel as well as the type and operating conditions of the combustor. Published emission data for alternative fuels burned in these types of combustion systems are limited and difficult to summarize due to variations in biodiesel and syngas configurations, feedstock, extent and nature of fuel



Figure 5: B20 blend at $\phi=1$.

cleanliness, and combustor configuration and operation [1]. However, based on well-established understanding of combustion chemistry and results from laboratory experiments, it is possible to estimate and understand pollutant formation during combustion of these fuels. In the experimental results shown at Figs. 7 to 14, a global overview can be seen for all the measurements taken throughout the experimental tests. The numerous emission results are compared to equilibrium values that were calculated using commercial software (GASEQ) at adiabatic flame temperature for the two baselines: methane for gaseous fuels and diesel for liquid fuels in order to ensure data validation. In addition, the results displayed in this study were averaged and summarized in a compact format for maximum information. Only the main pollutants are presented at different scales – wet, dry, and corrected to 15% O₂ on a dry basis – depending on their relevance.

Water Vapor, Carbon Dioxide and Oxygen. Water vapor (Fig. 7) and CO₂ (Fig. 9) concentrations increase almost linearly with equivalent ratio (ϕ) while the oxygen (Fig. 8) decreases to 0% at an equivalent ratio of 1 when all the air is consumed by the fuel. These 3 indicators are in good agreement with the theoretical trends we should get for emissions. It can also be observed that the gaseous fuels generate the greater amount of water vapor for those mixtures composed with the largest proportion of hydrogen and methane. In our case, S3 and S6 are composed of 50% hydrogen and generate the most water vapor compared to S1 and S4 with 25% hydrogen and a very low methane level.

Regarding the amount of oxygen left following combustion, the gaseous fuels seem to follow closely the theoretical values. On the other hand, the experimental measurements for liquid fuels give slightly higher O₂ concentrations, suggesting local excess air at the measured points. It should be also noted that these O₂ values were calculated based on a carbon/oxygen balance since the Zr-O₂ analyzer could not be activated for safety issues; this can add uncertainty to these values.

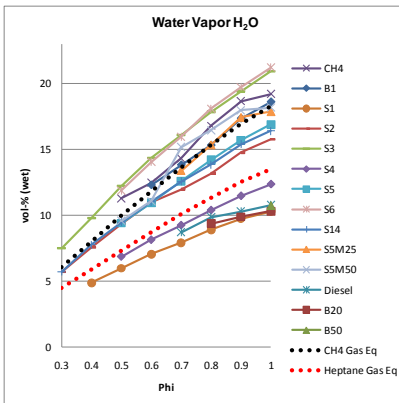


Figure 7: H₂O vs. ϕ .

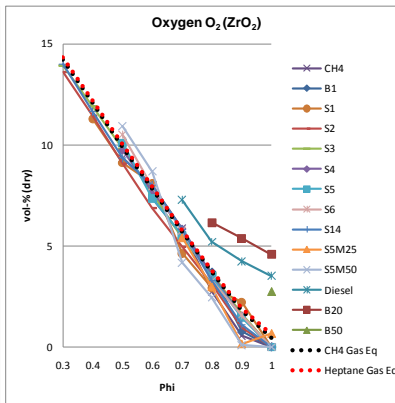


Figure 8: O₂ vs. ϕ .

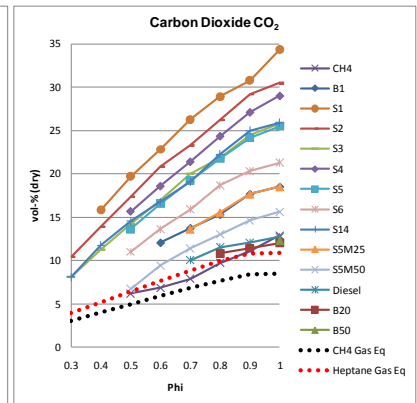


Figure 9: CO₂ vs. ϕ .

Nitrogen Oxides. NO_x is a collective term to describe several oxides of nitrogen that are important in combustion systems. The primary NO_x component of interest during the combustion of syngas is NO, especially for its strong contribution. NO emissions during combustion result primarily from two different mechanisms: fuel NO formation and thermal NO formation. A third mechanism, prompt NO formation, is responsible for a much smaller fraction of the overall NO_x emissions.

Thermal NO arises from the oxidation of molecular nitrogen (N₂) in the combustion air. These reactions involve radical species (O, N, H, OH) that are initially formed through decomposition or abstraction reactions. Due to the inherent stability of the N₂ molecule, considerable energy is required to oxidize N₂, and thus thermal NO is only formed in appreciable quantities at elevated combustion temperatures around ~1 500°C which is more than our case.

Indeed, NO formation is found to peak close to the fuel-lean side of stoichiometric ϕ . This is a consequence of the competition between fuel and nitrogen for the available oxygen. Although the combustion temperature is higher on the slightly rich side of stoichiometric ϕ , the available oxygen is then consumed preferentially by the fuel [3]. The exponential dependence of thermal NO on flame temperature is demonstrated in Fig. 10. This figure shows that NO production declines very rapidly as temperatures are reduced at

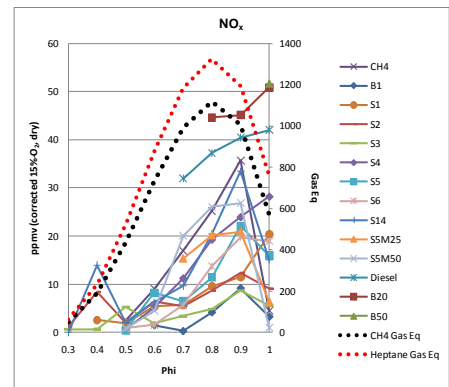


Figure 10: NO_x vs. ϕ .

low equivalence ratio ($\phi \cong 0.6$). Thermal NO is dominated by temperature effect consequently fuel composition can influence temperature especially when the gaseous mixture has a large proportion of CO₂ like B1, S1, S2, S3; thereby the lowest NO_x emissions. CO₂ is an inert gas so it does not participate in the combustion process. Consequently CO₂ reduce peak flame temperature by diluting and absorbing heat from the combustion product.

Of special interest in this figure is that the well-known difference in NO_x emissions between liquid and gaseous fuels diminishes with an increase in flame temperature. The reason for this is when burning liquid fuels there is always the potential for near-stoichiometric combustion temperatures, and consequently high NO_x formation, in local regions adjacent to the fuel drops, although the average equivalence ratio throughout the combustion zone may be appreciably less than stoichiometric. With an increase in the equivalence ratio, the bulk flame temperature becomes closer to the stoichiometric value, so that local conditions around the fuel drop have less influence on the overall combustion process and the NO_x emissions begin to approximate those produced by gaseous fuels when burning at the same equivalence ratio. Combustor residence time can also influence NO_x emissions which can increase with a longer residence time, except for very lean mixtures ($\phi \cong 0.4$), for which the rate of formation is so low that it becomes fairly insensitive to time. From our experimental results, this effect on NO formation seems to be related to the amount of hydrocarbon content in the fuel mixture. In fact, fuels generating the largest amount of NO_x are the diesel/biodiesel blends, CH₄ and S5M50. As hydrocarbon-content fuels are introduced, their higher flame temperature promote additional prompt NO formation.

Carbon monoxides in syngas combustion products has two primary sources: unburned syngas CO, resulting from inefficient mixing that yields equivalence ratios outside the ignition range, and incomplete combustion of hydrocarbon species in the syngas. When a combustion zone is stoichiometric or moderately fuel-lean, significant amounts of CO will also be present due to the dissociation of CO₂. In practice, CO emissions are found to be much higher than predicted from equilibrium calculations and to be highest at low-power conditions, where burning rates and peak temperatures are relatively low. This is in conflict with the predictions of equilibrium theory and it suggests that much of the CO arises from incomplete combustion of the fuel, probably caused by an inadequate burning rate in the quartz tube (combustor) due to a fuel/air ratio that is too low and/or insufficient residence time [4].

From our experimental results displayed in Fig. 11, CO emissions diminish with an increase in the equivalence ratio, reaching minimum values around $\phi \cong 0.5\sim 0.6$ depending on the fuel, any further increase in the equivalence ratio causes CO emissions to rise. These trends are typical of those observed for other types of combustion systems. The high levels of CO at low equivalence ratios are due to the slow rates of oxidation associated with low combustion temperatures. An increase in the equivalence ratio raises the flame temperature, which accelerates the rate of oxidation so that CO emissions decline. However, at temperatures higher than around 1500°C which is by far our case, the production of CO by chemical dissociation of CO₂ starts to become very significant.

Regarding the liquid fuels, CO emissions seem to follow an opposite path with respect to gaseous fuels. In fact, CO emissions increase while the equivalence ratio increases. The main effect of mean drop size on CO emissions stems from its strong influence on the volume required for fuel evaporation. At low equivalent ratio, where these emissions attain their highest concentrations, a significant proportion of the total combustion volume is occupied by fuel evaporation. Consequently, less volume is available for chemical reaction.

Unburned Hydrocarbons and Soot. UHCs include fuel that emerges from the combustor in the form of drops or vapor, as well as the species of lower molecular weight resulting from thermal degradation of the parent fuel. UHCs are normally associated with poor atomization, inadequate burning rates, or any combined effects. The reaction kinetics of UHC formation are more complex than for CO formation, but it is generally found in much the same way that the factors influencing CO emissions also influence UHC emissions [4]. Regarding unburned hydrocarbon levels, the measures recorded by the FID as well as the FTIR show relatively low UHC emissions for all gaseous fuels. In fact, UHCs never really exceeded more than 10 ppm. These good results are likely due to the high swirl capabilities of the fuel injector to ensure excellent mixing of the fuel with air. However, limitations

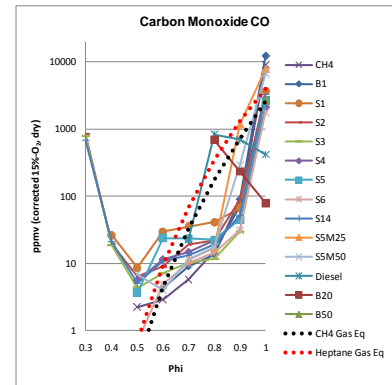


Figure 11: CO vs. ϕ .

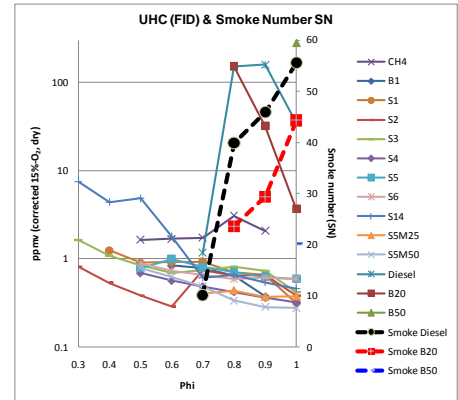


Figure 12: UHC & smoke vs. ϕ .

have been reached with liquid fuels. Indeed, high spray droplets impingements on the combustor walls have certainly interfered in the combustion process and affected the emissions in this way. Therefore, the amount of soot generated by diesel and bio-diesel is quite impressive especially at stoichiometric ϕ . Exhaust smoke is caused by the production of very fine soot particles in fuel-rich regions of the flame that are close to the fuel spray. These are the regions in which recirculating burned products move upstream toward the fuel injector, and local pockets of fuel vapor become enveloped in oxygen-deficient gases at high temperature. In these fuel-rich zones, soot is produced in considerable quantities. Analysis of the soot found in exhaust gases shows that it consists mostly of solid carbon (96%) and a mixture of hydrogen, oxygen, and other elements. As shown on Fig. 12, the smoke number increases very fast as we get closer to stoichiometric ϕ . The swirl effect has a very strong effect on the soot profile. Indeed, the solid carbon being relatively heavy compared to combustion gases has a tendency to be thrown from the center toward the combustor walls (centrifugal force). Consequently, this results in a very high and quasi saturated smoke number (~ 100) on the radial points and a relatively low smoke number at the center because of the high swirl effect.

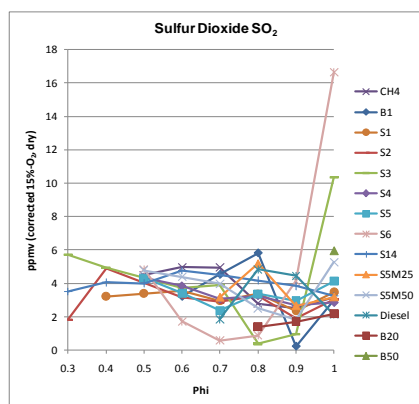


Figure 13: SO_2 vs. ϕ .

Sulfur Species. The primary sulfur component in syngas is hydrogen sulfide, which may exceed a concentration of 2% for sulfur-rich fuels. Smaller concentrations of other reduced sulfur compounds such as carbonyl sulfide, mercaptans, dimethyl sulfide, dimethyl disulfide, and carbon disulfide may also exist [4]. Because the gas entering the turbine is nearly sulfur-free, emissions of sulfurous compounds are relatively low (Fig. 13).

For syngas fired in internal combustion engines, sulfur species in the syngas are oxidized primarily to SO_2 . Some of the SO_2 will undergo further oxidation to form SO_3 . In systems with inefficient mixing of the air and syngas, fuel-rich regions or flow streams may exist. Under such circumstances, very little oxygen is available for complete combustion to SO_2 . Any reduced sulfur species remaining after all oxygen is consumed exit the system in a reduced form such as H_2S . Consequently, the partitioning of gaseous sulfur emissions between oxidized species (SO_2 and SO_3) and reduced species depends on the combustor performance and gas mixing.

5. Summary and Conclusions

The goal of this study is to characterize alternate liquid and gaseous fuels on a generic combustor with emission and smoke measurements and operability indicators such as ignition, lean blowouts, flame stability, and temperatures. This effort was pursued in response to growing interest to add flexibility in burning biofuels considering very limited information available regarding the effects of alternate fuels on pollutant emissions. From the experimental point of view, the test rig is not fully adequate for liquid fuel combustion. Massive droplet accumulations on the wall have certainly affected the combustion process. Maybe an intermediate size quartz tube would have prevented this issue by increasing the distance between the tube walls and the fuel spray. Moreover, the high accumulations of black soot along the quartz tube walls have likely affected emission measurements. Working conditions for the fuel injector are far from reel conditions in a gas turbine combustor with only the primary zone and the missing feed hole in the liner that normally promote further mixing and prevent larger droplets from reaching the combustor walls.

Concerning the gaseous fuel experiments, the tests were much simpler with almost no soot formation. Emission measurements show that S3 and S6 seem the most promising fuels regarding the relatively low NO_x , CO, and UHCs emissions generated and their very competitive Wobbe Index (Fig. 14) compared to baseline.

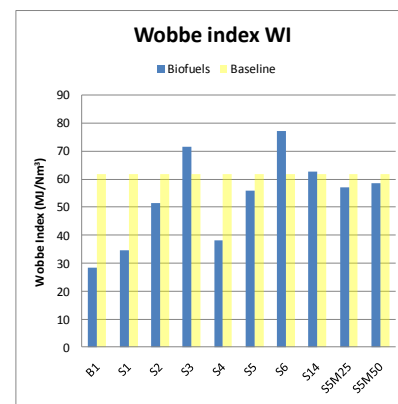


Figure 14: Wobbe index.

Acknowledgments

This work could not have been completed without the help and financial support of Rolls-Royce Canada, MITACS, NSERC and CRIAQ.

References

- [1] M. Youssef, J. Agou, A. deChamplain, B. Paquet, "Comparative Study for Biodiesel Properties and Standards for Gas Turbine", The Combustion Institute Canadian Section (CICS) (2012)
- [2] A. Barnwal, "Combustion Properties of Biologically Sourced Alternative Fuels", MSc. thesis, University of Toronto, ON, Canada, 2012.
- [3] A. Lefebvre, D. Ballal, "Gas Turbine Combustion – Alternative Fuels and Emissions", CRC Press, Florida, 2010, p.359.
- [4] T. Lieuwen, V. Yang, R. Yetter, "Synthesis Gas Combustion", CRC Press, Florida, 2010.